

Nuclear Magnetic Resonance of Oriented ^{196}Au , ^{198}Au , and ^{200m}Au †

F. Bacon, G. Kaindl,* H.-E. Mahnke,‡ and D. A. Shirley

Department of Chemistry and Lawrence Berkeley Laboratory, University of California, Berkeley, California 94720

(Received 10 November 1972)

Thermal equilibrium nuclear orientation was employed to orient nuclei of ^{196}Au , ^{198}Au , and ^{200m}Au as dilute impurities in nickel and iron at temperatures down to 4 mK. The degree of nuclear orientation was determined from the anisotropy of γ radiation emitted from the oriented nuclei. For Ni(^{200m}Au) both the magnetic hyperfine interaction $|\mu H| = (7.65 \pm 0.30) \times 10^{-18}$ erg and the magnetic hyperfine splitting $|\mu H/I| = (6.473 \pm 0.012) \times 10^{-19}$ erg were determined from an analysis of the temperature dependence of γ -ray anisotropies and by nuclear magnetic resonance on oriented nuclei (NMR/ON), respectively. As a result the spin I and the magnetic moment μ of the isomeric state could be derived as $I^\pi = 12^{(-)}$ and $\mu(12^-) = (\frac{1}{2}) (6.10 \pm 0.20) \mu_N$. From the measured anisotropies of five γ rays originating from the β^- decay of ^{200m}Au , spins and multipolarities could be assigned in the ^{200}Hg decay scheme. Nuclear magnetic resonance was also observed on oriented ^{196}Au and ^{198}Au in nickel at frequencies of 58.3 ± 0.4 MHz and 58.5 ± 0.4 MHz, respectively. The hyperfine interaction for Ni(^{197}Au), measured previously by spin echo, and our result for Ni($^{196},^{198}\text{Au}$) agree with the known atomic hyperfine anomalies between ^{197}Au and $^{196},^{198}\text{Au}$ only if the hyperfine field is assumed to have a noncontact contribution. For Ni($^{196},^{198}\text{Au}$) with $H_{\text{hf}} = (-)260.8 \pm 1.3$ kOe, the contact part is then found to be $H_c = -367 \pm 70$ kOe, with the noncontact contribution amounting to $H_{\text{nc}} = +106 \pm 70$ kOe. The angular distributions of several γ rays are in excellent agreement with a decay scheme proposed by Cunnane *et al.*, in which they found negative-parity levels of spins 5, 7, 9, and 11 at energies of 1852, 1963, 2144, and 2642 keV, respectively, in ^{200}Hg .

I. INTRODUCTION

Thermal equilibrium nuclear orientation, combined with nuclear magnetic resonance on oriented nuclei (NMR/ON), has recently been used successfully for the study of static and dynamic hyperfine interaction parameters of dilute impurities in ferromagnetic host metals.¹⁻³ This technique is especially useful when applied to high-spin isomeric states with half-lives of at least several hours, though only very few studies have been published up to now.⁴⁻⁶ Both the size of the magnetic hyperfine interaction and the spin of the oriented nuclear state can be obtained in this way.⁵

We have applied this technique to the 18.7-h isomer of ^{200}Au ,⁷ which is expected to be an analog of the well-known $I^\pi = 12^-$ isomeric state of ^{196}Au , for which spin and magnetic moment have previously been measured by the atomic beam method⁸ and by the nuclear orientation technique,⁹ respectively. A similar long-lived isomeric state with a half-life of 49 ± 2 h has recently been found in ^{198}Au .^{10, 11} In the present paper we report on results of a measurement of the temperature dependence of the anisotropy of nuclear γ rays emitted from oriented ^{200m}Au in nickel and iron, and of an NMR/ON experiment on ^{200m}Au in nickel. Both the spin and the magnetic moment of the isomer could be derived, providing evidence for its analogy with ^{196m}Au . In addition some spins and multipolarities could be assigned in the ^{200}Hg decay scheme from an analy-

sis of the anisotropies of five γ rays originating from the β^- decay of ^{200m}Au .

In another experiment, we have measured the magnetic hyperfine interaction of ^{196}Au and ^{198}Au in nickel by the NMR/ON technique. These results are helpful for the derivation of the nuclear g factor of ^{200m}Au from the measured nuclear magnetic resonance frequency, and they also provide a means for separating the hyperfine field of Ni($^{196},^{198}\text{Au}$) into a contact and a noncontact part. For this purpose, the present results for Ni($^{196},^{198}\text{Au}$) are compared with the hyperfine interaction measured previously for Ni(^{197}Au) by the spin-echo method.¹² It is found that the hyperfine fields derived from the measured interactions show differences which do not compare with the known atomic hyperfine anomalies between these nuclei, if the hyperfine fields are assumed to have pure contact character. The discrepancy can be resolved by including a noncontact part of the hyperfine field, which should not give rise to a hyperfine anomaly. The same method has previously been applied to the analysis of the hyperfine field of ^{198}Au in iron.¹³ Possible systematic errors inherent in this method due to unresolved electric quadrupole splitting are discussed, and the NMR results for noncontact hyperfine fields are compared with the results of Mössbauer experiments for ^{193}Ir in iron, cobalt, and nickel.

Following a brief description of the experimental procedure in Sec. II, the NMR/ON results for

^{196}Au and ^{198}Au in nickel will be presented in Sec. III A. In Sec. III B the NMR/ON results for ^{200m}Au in nickel are given, followed in Sec. III C by the results of the study of the temperature dependence of γ -ray anisotropies. Details of the analysis, and a discussion, are presented in Sec. IV.

II. EXPERIMENTAL PROCEDURE

A. Methods

In the present work nuclear polarization was achieved by thermal equilibrium nuclear orientation via magnetic hyperfine interaction at dilute impurities of gold in ferromagnetic iron and nickel. The technique for measuring the degree of nuclear orientation is based on the fact that nuclear radiations may be emitted from oriented nuclei with an anisotropic angular distribution. The observation of the anisotropy of γ radiation, in particular, can provide a useful tool for determining the degree of nuclear orientation. The angular distribution of γ rays with respect to the axis of quantization can be described by an equation of the form¹⁴

$$W(\theta) = 1 + \sum_k B_k U_k F_k Q_k P_k(\cos\theta), \quad (1)$$

where P_k are the Legendre polynomials and θ represents the angle between the direction of γ -ray emission and the quantization axis (in the present case identical with the direction of magnetization). The maximum value of k is determined by the spins of the nuclear states and by the γ -ray multipolarities. If parity violating admixtures in the pertinent nuclear states, and hence parity impurities in the γ -radiation field, can be neglected, only even values of k are permitted. With this assumption only terms with $k=2$ and $k=4$ were taken into account in the present work. The F_k are the angular distribution coefficients for the observed γ transition, the U_k are parameters describing the reorientation due to unobserved preceding decays, and the Q_k correct for the finite solid angle of the detector. The orientation of the initial state is described by the orientation parameters B_k , which are functions of the nuclear substate populations. The B_k parameters are quite insensitive to spin, depending almost entirely on the ratio of the total hyperfine interaction μH_{eff} to the thermal energy kT . Therefore the analysis of the temperature dependence of γ -ray anisotropies yields the magnetic hyperfine interaction μH_{eff} of the oriented nucleus.

Nuclear magnetic resonance on oriented nuclei (NMR/ON) can be detected by a change in the γ -ray anisotropy, caused by radiofrequency-induced transitions between the nuclear sublevels. From the resonance frequency ν a precise value of the magnetic splitting energy is obtained, which is

given by

$$h\nu = \mu H_{\text{eff}}/I. \quad (2)$$

A combination of the results of both measurements therefore yields directly a value of the spin of the oriented nuclear state.

B. Sample Preparation

The gold isotopes were produced by irradiating metallic platinum foils with 18-MeV deuterons or 35-MeV α particles. The targets had isotopic composition 5.8% ^{194}Pt , 13.6% ^{195}Pt , 36.2% ^{196}Pt , and 44.4% ^{198}Pt . Deuteron irradiation resulted in ^{196}Au and ^{198}Au via the $^{196}\text{Pt}(d, 2n)$ and $^{198}\text{Pt}(d, 2n)$ reactions, while ^{198}Au and ^{200m}Au were dominantly produced by α bombardment. The gold activity was separated carrier free from the platinum target by the standard ethyl acetate separation technique. After electrodeposition of the gold onto a nickel foil of 99.999% purity, the sample was melted several times in a hydrogen atmosphere. Foils were prepared from the Ni(Au) samples by cold rolling and annealing. For the NMR experiments the final thickness of the foils was adjusted to approximately 20 000 Å. Sources used for measuring the temperature dependence of γ -ray anisotropies also contained ^{60}Co activity for thermometry. The Fe(Au) samples were prepared in a similar way.

C. Apparatus

The samples were attached with Bi-Cd solder to the copper fin of an adiabatic demagnetization apparatus. Using cerium magnesium nitrate (CMN) as a cooling salt, temperatures down to 3 mK were reached. The relevant parts of the apparatus are shown in Fig. 1. The cooling salt and the copper fin were surrounded by copper heat shields which were cooled by potassium chromium alum (CA). A superconducting Helmholtz pair was employed to magnetize the samples in a homogeneous polarizing field H_0 . For the NMR experiments an rf field H_1 was applied perpendicular to H_0 . The amplitude of the rf field was measured during the experiment by means of a pickup coil. γ rays were detected along and perpendicular to the polarizing field.

For the measurement of the temperature dependence of γ -ray anisotropies, γ -ray spectra were taken for periods of 15 min with high resolution Ge(Li) diodes as the sample warmed up to 1 K over a typical period of 8 h. After corrections were made for background and exponential decay, the anisotropies of the different γ lines were obtained. The successive lattice temperatures were determined from the anisotropy of the 1173- and

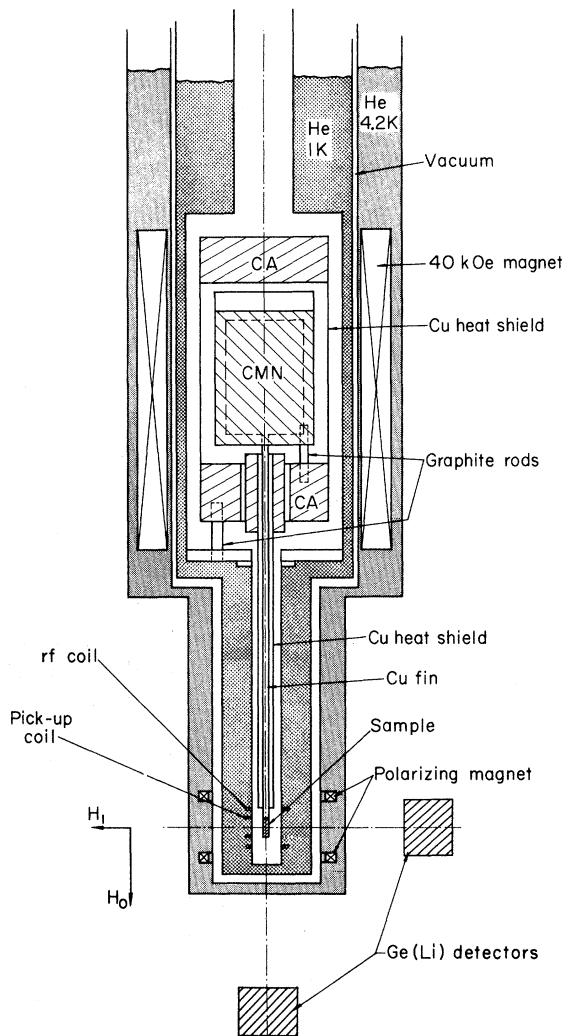


FIG. 1. Relevant parts of the demagnetization apparatus with source and detector arrangements.

1333-keV γ lines of ^{60}Co . In these experiments H_0 was 4.0 kOe.

In the NMR/ON experiments, 7.6×7.6 -cm NaI(Tl) detectors were employed in order to get higher counting rates. The intensities of the various γ lines observed along the polarizing field were measured as functions of the frequency of the applied rf field, which was modulated in sawtooth form over a bandwidth of 2 MHz with a modulation frequency of 100 Hz; the amplitude of the rf field was in the range of 0.2 to 0.6 mOe.

III. RESULTS

A. NMR/ON Results for $\text{Ni}(^{196}\text{Au})$ and $\text{Ni}(^{198}\text{Au})$

Using the ^{196}Au and ^{198}Au activities produced in the same target by deuteron irradiation, nuclear

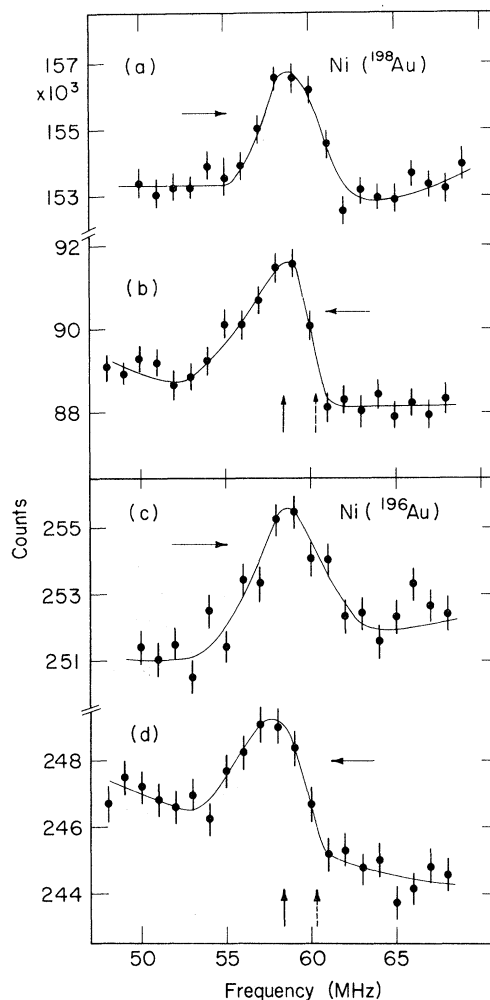


FIG. 2. NMR/ON resonance of ^{198}Au (upper part) and ^{196}Au (lower part) in nickel measured for increasing (a and c) and decreasing (b and d) frequencies. The solid vertical markers indicate the measured line positions, while the dashed ones show the line positions if the hyperfine anomaly for Au in nickel were the same as for the free Au atom.

magnetic resonance could be observed simultaneously on the oriented 2^- ground states of ^{196}Au and ^{198}Au dissolved in nickel. The γ lines used for detecting the resonance were the 412-keV transition in ^{198}Hg following the β^- decay of ^{198}Au , and the 356-keV transition in ^{196}Pt following the electron-capture decay of ^{196}Au . The intensities of these γ rays observed along the polarizing field as functions of the frequency of the rf field are shown in Fig. 2.

Although the frequency was varied in steps of 1 MHz with a total time span between adjacent data points of 4.25 min, the resonance curves measured for increasing frequencies (Fig. 2, curves a and c)

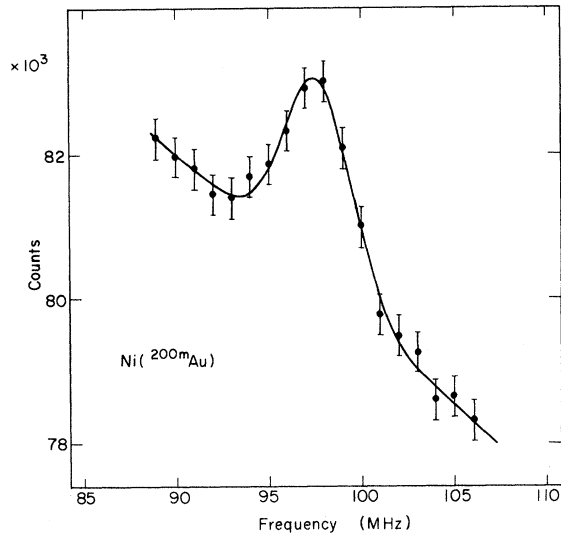


FIG. 3. NMR/ON resonance of ^{200m}Au in nickel, observed via the frequency dependence of the summed intensities of the 498-, 580-, and 760-keV γ lines at zero degrees. The solid line represents the result of a least-squares fit of the data to a Gaussian line with linear background.

and for decreasing frequencies (Fig. 2, curves b and d) are shifted relative to each other and are quite asymmetric. This is a consequence of the rather long nuclear spin lattice relaxation time,

which was determined as $T_1' = 3 \pm 1$ min, using a single exponential fit.²

Because of the asymmetry of the resonance lines the resonance frequencies were determined from the averages of the leading edges, yielding for

$$\text{Ni}(^{196}\text{Au}): \nu = 58.3 \pm 0.4 \text{ MHz},$$

and for

$$\text{Ni}(^{198}\text{Au}): \nu = 58.5 \pm 0.4 \text{ MHz}.$$

A similar resonance curve for $\text{Ni}(^{198}\text{Au})$ was additionally measured with a source prepared from the activity obtained in the α irradiation and used for the ^{200m}Au experiment. While the anisotropy of the 412-keV γ line decreased when entering the resonance, no effect was observed within this frequency range on the γ lines originating from the ^{200m}Au decay. The possibility of warming up the sample by a coil resonance could therefore be ruled out.

B. NMR/ON Results for $\text{Ni}(^{200m}\text{Au})$

The β^- decay of ^{200m}Au is followed by six major γ transitions of energies 181, 256, 368, 498, 580, and 760 keV. The result of our nuclear orientation experiments showed that only the 256-keV γ line has positive anisotropy, indicated by increasing intensity along the polarizing field with decreasing temperature. For all the other γ transitions the intensities at $\theta = 0^\circ$ decreased drastically when the

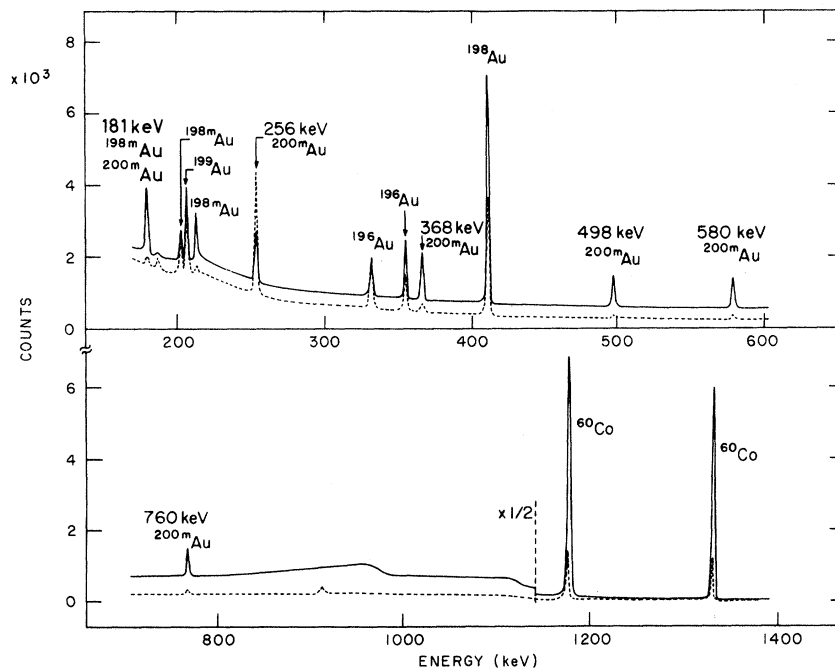


FIG. 4. γ -ray spectra of Au isotopes in iron at a lattice temperature of 5 mK (dashed line) and at ≈ 1 K (solid line), taken at 0 degrees relative to the external polarizing field.

sample was cooled (see Fig. 4).

Therefore, the nuclear magnetic resonance of Ni(^{200m}Au) was observed by recording the sum of the intensities of the 498-, 580-, and 760-keV γ lines at zero degrees as a function of the frequency of the applied rf field. The result is presented in Fig. 3. When the resonance curve was measured with increasing or decreasing frequency, no shift of the resonance peak was observed. This is in agreement with a short nuclear spin lattice relaxation time T_1' , which was found to be shorter than 10 sec in the temperature range between 4 and 10 mK. A Gaussian line with linear background was least-squares-fitted to the data points, resulting in the resonance frequency

$$\nu = \mu H_{\text{eff}} / \hbar I = 97.7 \pm 0.2 \text{ MHz},$$

which corresponds to $(6.473 \pm 0.012) \times 10^{-19}$ erg. No resonance was detected with an unmodulated radio frequency field, again ruling out the possibility of a coil resonance.

C. Temperature Dependence of the Anisotropies of the ^{200m}Au γ Lines

Although the ^{200m}Au activity produced by α irradiation was contaminated with ^{196}Au , ^{196m}Au , ^{198}Au , ^{198m}Au , and ^{199}Au activities, the γ lines originating from the ^{200m}Au decay were well separated in the γ -ray spectrum. Figure 4 shows the relevant parts of the γ -ray spectra taken along the polarizing field when the Au nuclei were oriented at a lattice temperature of ~ 5 mK (dashed line), and 10 h later when the Fe(Au) sample was at ~ 1 K (solid line). The temperature dependence of the anisotropy was measured for the 256-, 368-, 498-, 580-, and 760-keV γ lines. The intensity of the 181-keV γ lines showed a decay time different from that of the other γ lines of the ^{200m}Au decay. This indicates an underlying line of nearly the same energy which could be identified as a transition in ^{198}Au ,

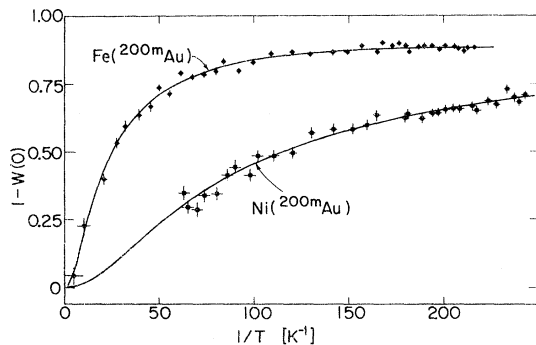


FIG. 5. Temperature dependence of the function $1-W(0)$ of the 368-keV γ rays of Fe(^{200m}Au) and Ni(^{200m}Au).

TABLE I. Results of the least-squares-fit analysis of the temperature dependence of the anisotropy of the 412-keV γ rays of Fe(^{198}Au) in comparison with values in the literature.

μH (10^{-18} erg)	U_2	U_4	Reference
3.50 ± 0.06	0.797 ± 0.022	0.261 ± 0.058	This work
3.437 ± 0.006	0.795 ± 0.007	0.347 ± 0.030	13, 15

originating from the decay of ^{198m}Au .¹¹

The anisotropy of the 368-keV γ line, measured along the polarizing field, is plotted in Fig. 5 versus the reciprocal lattice temperature for samples of Fe(^{200m}Au) and Ni(^{200m}Au). The solid lines represent least-squares fits of the data to the theoretical angular distribution function [Eq. (1) with $k = 2, 4$]. Since very little is known about the multipolarities of the transitions, the 0 and 90° spectra were fitted simultaneously, taking the products $U_2 F_2$ and $U_4 F_4$, the magnetic hyperfine interaction μH , and an amplitude factor for the 90° spectra as free parameters. The latter parameter was included to correct for possible intensity differences in the 0 and 90° spectra due to the background correction. As a test, the fit procedure was also applied to the anisotropy curve of the 412-keV γ line of Fe(^{198}Au). It yielded satisfactory agreement between the derived quantities and the known values from NMR/ON¹³ and NO¹⁵ studies, as demonstrated in Table I.

The Ni(^{200m}Au) data were additionally fitted under the assumption of various values for the spin of the isomeric state. The results for μH are given in Table II. While μH is practically independent of the assumed spin, an agreement with the NMR result is obtained only for a spin of $I = 12$. This is demonstrated in column 3 of Table II, in which the nuclear orientation results are compared with the NMR result. Because of the large spin, the sensitivity of this method is not as high as it was in the case of ^{195m}Pt , for which the same method was successfully applied to determine the spin of the isomeric state.⁵

TABLE II. Summary of fit results for μH obtained from the anisotropy curves for Ni(^{200m}Au), assuming various values for the spin of the isomeric state.

Spin I	μH (10^{-18} erg)	$(\mu H)_{\text{NO}} / (\mu H)_{\text{NMR}}$
11	7.60 ± 0.30	1.080 ± 0.040
12	7.65 ± 0.30	0.995 ± 0.040
13	7.71 ± 0.30	0.925 ± 0.040

With the spin established as 12, the anisotropy curves for $\text{Ni}(^{200m}\text{Au})$ were fitted once more in order to get more accurate values for the angular distribution coefficients $U_k F_k$ of the γ lines. Thereby the magnetic hyperfine interaction was set equal to the result of the NMR/ON experiment and kept constant during the fit. The results are summarized in Table III.

IV. DISCUSSION

A. Magnetic Hyperfine Field of Gold in Nickel

The ratio of the magnetic hyperfine structure constants of two nuclear levels in the same atomic environment, a_1 and a_2 , may differ from the ratio of the respective nuclear g factors. The hyperfine anomaly¹⁶ is defined by the relation

$$a_1/a_2 = (1 + {}^1\Delta^2)g_1/g_2. \quad (3)$$

Because of their different distributions over the finite size of the nucleus, the spin and orbital parts of the nuclear magnetic moment experience different magnetic fields from the contact part of the magnetic hyperfine interaction, provided that the atomic number is large enough for the contact field itself to vary over the nuclear volume. Thus the average field sensed by the moment depends on the nucleon distribution. If the deviation from the point dipole interaction is written in terms of the "single-level anomaly" ϵ , as

$$a = a_0(1 + \epsilon) \quad (4)$$

then the hyperfine anomaly can be expressed as

$${}^1\Delta^2 = \frac{\epsilon_1 - \epsilon_2}{1 + \epsilon_2}. \quad (5)$$

If the induced magnetic hyperfine fields at dilute impurities in ferromagnetic host lattices, such as $\text{Ni}(\text{Au})$, arise entirely from a Fermi contact interaction, the hyperfine anomaly determined with such internal fields should have the same value as the anomaly determined from the hyperfine structure

constants of free atoms, measured, e.g., by the atomic beam method. A difference in the anomalies such as that observed between the ground states of ^{198}Au and ^{199}Au ¹³ indicates the presence of noncontact contributions to the hyperfine field, provided that quadrupole effects can be neglected (see below). If we derive an effective hyperfine field H_{eff} from the measured interaction by dividing the average interaction μH_{eff} by the magnetic moment, the anomaly found in a ferromagnetic host can be expressed as

$$\frac{H_{1\text{eff}}}{H_{2\text{eff}}} = 1 + {}^1\Delta_{\text{host}}^2. \quad (6)$$

For the ground states of both ^{196}Au and ^{198}Au , in which the magnetic moments and the hyperfine anomaly have been determined by atomic beam studies,¹⁷ the moments differ by only $0.33 \pm 0.26\%$ and the hyperfine anomaly ${}^{196}\Delta^{198}$ was found to be zero within the limits of error (see Table IV). This result is reflected in the practically equal resonance frequencies observed in our NMR experiment. With the mean value of $\mu = 0.5897$ for the magnetic moment (corrected for diamagnetism) we derive an internal magnetic field for $^{196,198}\text{Au}$ in nickel of $H_{\text{hf}} = (-)260.8 \pm 1.3$ kOe, after correcting for the external polarizing field. This value of the hyperfine field may be compared with the one measured for ^{197}Au in nickel as $H_{\text{hf}} = -292 \pm 6$ kOe. (Originally the authors of the spin-echo experiment on ^{197}Au ¹² quoted a value of $H_{\text{hf}} = -294 \pm 4$ kOe, derived by using a moment of $\mu = 0.1439$. In order to be consistent we have recalculated the field by taking the moment $\mu = 0.1435$ as it was used in the analysis of the atomic beam results¹⁸ and correcting it for diamagnetism.)

From the ratio of the fields we can determine a hyperfine anomaly for the ground states of ^{197}Au and ^{198}Au in nickel of

$${}^{197}\Delta_{\text{Ni}}^{198} = +(12.0 \pm 2.3)\%,$$

which is considerably larger than the anomaly for

TABLE III. Summary of results for the anisotropy coefficients $U_2 F_2$ and $U_4 F_4$ of the strongest γ lines in the decay of ^{200m}Au .

γ line (keV)	$U_2 F_2$	$U_4 F_4$
256	0.253 ± 0.012	0.009 ± 0.013
498	-0.342 ± 0.015	-0.130 ± 0.018
760	-0.342 ± 0.020	-0.126 ± 0.025
580	-0.353 ± 0.016	-0.112 ± 0.020
368	-0.323 ± 0.010	-0.126 ± 0.012

TABLE IV. Calculated and measured hyperfine anomalies ${}^a\Delta^a$ for different Au isotopes. The calculated single-level anomalies ϵ are given in column 2.

A	ϵ		${}^{197}\Delta^a$		${}^{198}\Delta^a$	
	Calc.	Calc.	Exp.	Calc.	Exp.	
197	10.3	-9.0	-7.96 ± 0.08^a	
198	0.4	+9.9	$+8.53 \pm 0.08^a$	
196	0.4	+9.9	$+8.72 \pm 0.24^b$	0.0	$+0.2 \pm 0.3^b$	
199	4.3	+5.8	$+3.7 \pm 0.2^a$	-3.8	-4.5 ± 0.3^a	
200m	-1.9	+12.5	...	+2.3	...	

^a Reference 18.

^b Reference 17.

pure contact interaction in the free atom¹⁸

$${}^{197}\Delta^{198} = +(8.53 \pm 0.08)\%$$

This discrepancy can be interpreted as indicating the presence of both a contact and a noncontact contribution to the hyperfine field for a point nucleus,

$$H_{\text{hf}}^0 = H_{\text{c}}^0 + H_{\text{nc}}^0.$$

Since the anomaly arises from H_{c} alone, a relation of the form

$$H_{\text{c}}/H_{\text{hf}} \cong \Delta_{\text{Ni}}/\Delta_0,$$

would be expected to apply to the Ni(Au) case. There is not enough information to derive unique values of H_{c} and H_{nc} . For that purpose we would have to know the values of ϵ in one isotope. Making the reasonable assumption that most of the ${}^{197}\Delta^{198}$ and ${}^{197}\Delta^{196}$ anomalies arise from distributed nuclear magnetism in ${}^{197}\text{Au}$ (i.e., that ${}^{197}\Delta^{196, 8} \cong \epsilon_{197}$), we can use $H_{\text{hf}}\text{Ni}({}^{196, 198}\text{Au})$ as the "point nucleus" field H_{hf}^0 . Thus

$$H_{\text{c}} = \frac{{}^{197}\Delta^{198}}{{}^{197}\Delta^{196}} (-260.8 \text{ kOe}) = -367 \pm 70 \text{ kOe},$$

and

$$H_{\text{nc}} = +106 \pm 70 \text{ kOe}.$$

The large size of H_{c} , and its sign, confirms earlier expectations that H_{hf} for $5d$ elements dissolved in ferromagnets arises mainly from the Fermi contact interaction. While this is a valuable result, it is certainly not unexpected.

Several other cases of positive values for H_{nc} have been reported for $5d$ impurities in iron, cobalt, and nickel.^{13, 19-21} The data are summarized together with the present result in Table V. Mössbauer results obtained with the 73-keV γ transition of ${}^{193}\text{Ir}$ yielded positive values of H_{nc} for Fe, Co, and Ni.¹⁹⁻²¹ Within the large error bars they agree with the H_{nc} values for Fe(${}^{198}\text{Au}$)¹³ and the present result for Ni(${}^{196, 198}\text{Au}$) derived

from NMR/ON experiments. Obviously, H_{nc} decreases with decreasing induced hyperfine field from iron to nickel hosts.

The H_{nc} term is of considerable interest, as it probably arises from the orbital angular momentum of the Au $5d$ electrons. That l should not be completely quenched for this case is not surprising, because the $5d_{3/2} - 5d_{5/2}$ free-atom spin-orbit splitting in this region is 1.5–2 eV, while the coupling strength of the crystal lattice may be taken as ~ 5 eV (the $5d$ bandwidth in metallic gold) or less. Since the gold $5d$ spins are polarized by the ferromagnetic lattice (and in turn contribute to H_{c} through spin-exchange polarization of the filled inner s shells), one would expect the $l \cdot s$ interaction to lead to an incomplete quenching of the orbital angular momentum, and the expectation value of l_z should be nonzero. The positive sign of H_{nc} indicates that $\langle l_z \rangle_{5d}$ and $\langle s_z \rangle_{5d}$ have the same sign (i.e., l and s are polarized parallel). If this were free atomic gold, in the configuration $5d^9 6s^2$, the j - j coupling populations would be $(5d_{3/2})^4(5d_{5/2})^5 6s^2$, and the unpaired $5d$ spin \vec{s} would indeed be parallel to \vec{l} . Such a simple picture is not adequate for the gold atom in a nickel lattice, but this may be the essential reason that \vec{l} and \vec{s} are parallel. It would be premature to interpret the magnitude of H_{nc} at this time, since the values are still not accurate enough. However, a hyperfine field of order of magnitude 10^6 Oe is usually associated with one unit of orbital angular momentum, so that the H_{nc} fields reported here correspond to rather small values of $\langle l_z \rangle$.

Stone³ has pointed out that hyperfine anomalies measured by the NMR/ON method are subject to question because of a possible electric quadrupole interaction. In fact if $\langle l_z \rangle \neq 0$, it is very probable that the m_l states will be unequally populated, giving rise to a field gradient proportional to $\langle l_z^2 - \frac{1}{3}l(l+1) \rangle$. Lattice distortions could also contribute to the electric field gradient.

Such effects have been observed up to now only for ${}^{193}\text{Ir}$ and ${}^{191}\text{Ir}$ impurities in iron and nickel. Wagner and Potzel²¹ derived from the hyperfine spectrum of the 73-keV γ rays of ${}^{193}\text{Ir}$ in Fe and Ni values for the electric quadrupole coupling constant $P = eqQ/2 = -0.054 \pm 0.010$ mm/sec for Fe and -0.042 ± 0.006 mm/sec for Ni, corresponding to 3.2 ± 0.6 MHz and 2.5 ± 0.4 MHz, respectively. With $Q = +1.5 \pm 0.1$ b for the $\frac{3}{2}$ state of ${}^{193}\text{Ir}$ a negative value for eq is obtained. In reasonable agreement with the Mössbauer results, Aiga and Itoh²² have recently observed satellite lines in the NMR spectra of ${}^{191, 193}\text{Ir}$ in Fe and Ni, with separations of $|P| = 2.5$ MHz and 1.4 MHz for Fe and Ni, respectively.

Such an electric quadrupole interaction would

TABLE V. Noncontact hyperfine fields of Au and Ir impurities in Fe, Co, and Ni, derived from the results of NMR/ON and Mössbauer (M) experiments.

Host	Probe nucleus	H_{nc} (kOe)	Method	Reference
Fe	${}^{198}\text{Au}$	$+270 \pm 70$	NMR-ON	13
	${}^{193}\text{Ir}$	$+335 \pm 200$	M	19, 20
	${}^{193}\text{Ir}$	$+155 \pm 90$	M	21
Co	${}^{193}\text{Ir}$	$+149 \pm 80$	M	21
Ni	${}^{198}\text{Au}, {}^{198}\text{Au}$	$+106 \pm 70$	NMR-ON	Present result
	${}^{193}\text{Ir}$	$+52 \pm 50$	M	21

lead to an asymmetry of the NMR/ON spectrum and at very low temperatures, in the limit $1/T \rightarrow \infty$, to a shift of the resonance line by $\Delta\nu_{\max} = -\frac{3}{4}P$ for a spin of $I=2$. For a rough estimate of $\Delta\nu_{\max}$ we use the electric field gradient from Aiga's work with the negative sign, and $Q(2^-) \cong +0.85$ b for the quadrupole moment of the 2^- ground states of ^{196}Au and ^{198}Au . This value was obtained by assuming that these two nuclei have the same intrinsic quadrupole moment as the ground state of ^{197}Au . We then get $\Delta\nu_{\max} \cong +0.6$ MHz for $\text{Ni}(^{196,198}\text{Au})$, which cannot explain the observed resonance frequency. As indicated by the dashed vertical markers in Fig. 2 the resonance frequencies expected for pure contact interaction would be $\cong 2$ MHz larger than the experimental ones. In summary, a possible electric quadrupole interaction in this case is expected to be too small and of the wrong sign to explain the experimental resonance frequencies. However, such quadrupole effects must be taken into account in the interpretation of differences in hyperfine anomalies in terms of contact and noncontact magnetic hyperfine fields. At present, no quantitative distinction can be made between the effects, but it seems likely from the above estimate for the maximum quadrupole shift that the noncontact part of the magnetic hyperfine field of $\text{Ni}(\text{Au})$ is slightly larger than derived above. Obviously, a study of the temperature dependence of the resonance spectrum would be desirable. This could lead to a direct measurement of the electric quadrupole interaction including its sign, and therefore to a separation of both effects on the NMR/ON resonance line.

B. Magnetic Moment of ^{200m}Au

As demonstrated in the previous section, quite large differences are observed in the hyperfine fields for Au in nickel (and iron) due to the hyperfine anomaly. Within the framework of the Bohr-Weisskopf theory¹⁶ one can show that the main contribution to the anomaly arises from the $d_{3/2}$ ground state of ^{197}Au . Therefore it is probably realistic to use the hyperfine field value for ^{198}Au in the derivation of the magnetic moment of ^{200m}Au .

From the measured resonance frequency we can then derive a value for the g factor of

$$g = \pm 0.492 \pm 0.003.$$

Together with the determined spin of $I=12$, this leads to a magnetic moment of

$$\mu = (\pm 5.90 \pm 0.04)\mu_N.$$

This result is very similar to the moment found for the 12^- state of ^{198}Au ,⁹ so we may assume that the isomeric state in ^{200}Au is analogous to the 12^- state in ^{196}Au with a $[\pi h_{11/2}, \nu i_{13/2}]_{12^-}$ shell-

model configuration. By using the hyperfine field value of ^{198}Au we have neglected a possible anomaly $^{198}\Delta^{200m}$ between the ground state of ^{198}Au and the 12^- state of ^{200}Au . We can get an estimate for the possible correction from the Bohr-Weisskopf theory using the measured anomalies $^{196}\Delta^{197}$, $^{197}\Delta^{198}$, $^{197}\Delta^{199}$, and $^{196}\Delta^{198}$ (Refs. 17 and 18) as a check of its applicability.

For the odd-odd nuclei the proton and neutron fractions of spin and orbital parts of the total moment were calculated using the coupling rule and adjusting the spin g factors of proton and neutron to reproduce the measured moments. For ^{196}Au the experimental g factor of ^{197}Au , and for ^{198}Au the experimental g factor of ^{199}Au were taken for the proton state. For ^{200m}Au we used for the proton state $\mu(\pi_{11/2^-}) = 6.7\mu_N$ as calculated with the spin polarization procedure of Arima and Horie.²³ The calculations are summarized in Table IV. The single-level anomalies ϵ are presented in column 2, calculated and measured hyperfine anomalies with respect to ^{197}Au are given in columns 3 and 4, and anomalies with respect to ^{198}Au appear in columns 5 and 6. As pointed out above, by far the largest single level anomaly is calculated for the ground state of ^{197}Au .

Since the agreement between measured and calculated anomalies is satisfactory, the values for $^{197}\Delta^{200m}$ and $^{198}\Delta^{200m}$ can be taken as quite realistic figures for correcting the magnetic moment of ^{200m}Au . The corrected values of the magnetic moments of the 12^- state are given in Table VI. The uncorrected values, derived with the field values for ^{197}Au and ^{198}Au , appear in column 2, and the anomalies from Table IV are listed in column 3. The corrected values in column 4 were obtained by assuming pure contact interaction, while those given in column 5 include a correction for noncontact parts as derived above. Taking the value with the smaller correction, the final result is

$$\mu = (6.10 \pm 0.20)\mu_N,$$

for the magnetic moment of the 12^- state of ^{200}Au . The quoted error was estimated from the largest deviation between measured and calculated hyperfine anomalies (see Table IV) including the correction for a noncontact contribution to the hyper-

TABLE VI. Derivation of the magnetic moment of the 12^- state of ^{200}Au .

A	μ		μ	
	Uncor.	$A\Delta^{200m}$	Contact	Noncontact
197	5.27 ± 0.10	12.5	5.94	6.20
198	5.90 ± 0.04	2.3	6.04	6.10

fine field; the statistical error would be only $0.04\mu_N$. This moment is more than 10% larger than the moment of the corresponding 12^- state in ^{196}Au , which was recently determined by the NO technique as $\mu = (5.35 \pm 0.20)\mu_N$.⁹ The difference may arise from different contributions of the $i_{13/2}$ neutron component. Such an interpretation is suggested by the value of the magnetic moment of the $i_{13/2}$ state of ^{195}Pt which was found to be more than $0.4\mu_N$ smaller than the moments of the corresponding states in neighboring mercury isotopes.⁵

C. Decay Scheme of ^{200m}Au

In the decay of ^{200m}Au the 368- and 580-keV γ transitions are known to be $E2$ transitions deexciting the first 2^+ and 4^+ state of ^{200}Hg ,²⁴ respectively. From $\gamma\gamma$ and γe^- coincidence experiments Ton *et al.*²⁵ concluded that the 181-, 760-, and 580-keV γ lines follow the decay of a $T_{1/2} = 1.07$ -nsec level at 1888-keV excitation energy, while the 498- and perhaps the 256-keV transition precede this level; the relative order of the preceding transitions could not be established. Based on analogy with lower mass even mercury isotopes, a spin of 6^- or 7^- was assumed for the 1.07-nsec level in Ref. 25, with the 181-keV transition populating the 4^- or 5^- level, respectively, followed by the 760-keV transition to the 4^+ state.

From the γ -ray anisotropies determined in the present work, some spins and multiplicities can be assigned in the ^{200}Hg decay scheme. The experimental values for U_2F_2 and U_4F_4 are summarized in Table III. They clearly indicate that both the 498- and 760-keV transitions should be of the same type as the known 368- and 580-keV transitions, namely quadrupole with $\Delta I = -2$; i.e., $I_i = I_f + 2$. Furthermore, the anisotropy of the 256-keV transition is compatible only with a dipole character with $\Delta I = -1$. Taking into account the relative γ intensities of the cascading transitions, the 256-keV transition should be $E1$ and the 498-keV transition $E2$.

For the 1.707-MeV level, deexcited by the 760-keV γ line, a spin of 4 or 5, as previously assumed,²⁵ is definitely ruled out by the measured anisotropy requiring a spin of 6. It seems likely that this level has positive parity and the 760-keV transition hence $E2$ character. In lower even-mass Hg isotopes 6^+ states are known to exist between 1.7 and 1.8 MeV excitation energy.²⁶

For the rest of the decay scheme, spin-parity

assignments cannot be made with certainty from our results alone. However, Cunnane *et al.*²⁷ have recently proposed a decay scheme that the angular distributions in Table III can test rather rigorously. They proposed that ^{200m}Au decays to an 11^- state at 2642 keV in ^{200}Hg . This state would then decay by the cascade 11^- , 2642 keV (498 keV, $E2$) 9^- , 2144 keV (181 keV, $E2$) 7^- , 1963 keV. Two parallel cascades would deexcite this level to a 4^+ level at 947 keV. These are (111 keV, $E2$) 5^- , 1852 keV (904 keV, $E1$), and (256 keV, $E1$) 6^+ , 1707 keV (760 keV, $E2$).

The proposed decay scheme of Cunnane *et al.* is consistent in some detail with our results. That is, the 498- and 760-keV transitions' $E2$ multipolarity and spin change $\Delta I = -2$ is consistent, as discussed above. In our experiment the anisotropy of the 181-keV γ ray could not be evaluated quantitatively because of the presence of ^{198m}Au activity which has a line at 180.3 keV.^{10, 11} This line has a large negative anisotropy.¹¹ Taking into account the relative γ -ray intensities in the ^{198m}Au and ^{200m}Au decay schemes, the large negative anisotropy observed for the sum of the two γ lines (see Fig. 4) establishes that the 181.1-keV γ transition cannot have pure $E1$ character. It is, however, consistent with an $E2$, $\Delta I = -2$ transition as proposed by Cunnane *et al.*²⁷

No quantitative evaluation has been carried out for the anisotropy of the rather weak 904-keV γ line due to the large ^{60}Co background; but as one can see from an inspection of Fig. 4, this γ line exhibits a large positive anisotropy, in good agreement with the $E1$, $\Delta I = -1$ character that the decay scheme of Cunnane *et al.* would require. As indicated above, this decay scheme agrees well with the angular distribution of the 256-keV γ ray.

In summary, our results strongly confirm the decay scheme of Cunnane *et al.*, while flatly contradicting that of Ton *et al.* Thus we believe that the former is correct.

ACKNOWLEDGMENTS

The authors would like to thank Mrs. Winifred Heppler for her help in chemical separations and sample preparations. One of the authors (G.K.) gratefully acknowledges a postdoctoral fellowship by the Miller Institute for Basic Research in Science, and (H.E.M.) wants to thank the Deutscher Akademischer Austauschdienst for granting a North Atlantic Treaty Organization fellowship.

†Work performed under the auspices of the U. S. Atomic Energy Commission.

*Present address: Physik-Department, Technische

Universität, München, D-8046 Garching, Germany.

‡Present address: Hahn-Meitner-Institut für Kernforschung, D-1000 Berlin, Germany.

- ¹E. Matthias and R. J. Holliday, *Phys. Rev. Letters* **17**, 897 (1966).
- ²W. D. Brewer, D. A. Shirley, and J. E. Templeton, *Phys. Letters* **27A**, 81 (1968).
- ³N. J. Stone, in *Hyperfine Interactions in Excited Nuclei*, edited by G. Goldring and R. Kalish (Gordon and Breach, New York, 1971), p. 237.
- ⁴R. A. Fox, P. D. Johnston, C. J. Sanctuary, and N. J. Stone, in *Hyperfine Interactions in Excited Nuclei* (see Ref. 3), p. 339.
- ⁵F. Bacon, G. Kaindl, H.-E. Mahnke, and D. A. Shirley, *Phys. Rev. Letters* **28**, 720 (1972).
- ⁶G. Eska, E. Hagn, T. Butz, P. Kienle, and E. Umlauf, *Phys. Letters* **36B**, 328 (1971).
- ⁷K. Sakai and P. J. Daly, *Nucl. Phys.* **A118**, 361 (1968).
- ⁸Y. W. Chan, W. B. Ewbank, W. A. Nierenberg, and H. A. Shugart, *Phys. Rev.* **127**, 572 (1962).
- ⁹F. Bacon, G. Kaindl, H.-E. Mahnke, and D. A. Shirley, *Phys. Letters* **37B**, 181 (1971), and references therein.
- ¹⁰J. C. Cunnane and P. J. Daly, private communication.
- ¹¹F. Bacon, G. Kaindl, and H.-E. Mahnke, to be published.
- ¹²M. Kontani and J. Itoh, *J. Phys. Soc. Japan* **22**, 345 (1967).
- ¹³R. A. Fox and N. J. Stone, *Phys. Letters* **29A**, 341 (1969).
- ¹⁴R. J. Blin-Stoyle and M. A. Grace, in *Handbuch der Physik*, edited by H. Geiger and K. Scheer (Verlag von Springer, Berlin, 1957), Vol. 42, p. 555.
- ¹⁵W. P. Pratt, R. I. Schermer, and W. A. Steyert, *Phys. Rev. C* **2**, 608 (1970).
- ¹⁶A. Bohr and V. F. Weisskopf, *Phys. Rev.* **77**, 94 (1950).
- ¹⁷S. G. Schmelling, V. F. Ehlers, and H. A. Shugart, *Phys. Rev. C* **2**, 225 (1970).
- ¹⁸P. A. Vanden Bout, V. J. Ehlers, W. A. Nierenberg, and H. A. Shugart, *Phys. Rev.* **158**, 1078 (1967).
- ¹⁹G. J. Perlow, W. Henning, D. Olsen, and G. L. Goodman, *Phys. Rev. Letters* **23**, 680 (1969).
- ²⁰G. J. Perlow, in *Hyperfine Interactions in Excited Nuclei* (see Ref. 3), p. 651.
- ²¹F. E. Wagner and W. Potzel, in *Hyperfine Interactions in Excited Nuclei* (see Ref. 3), p. 681; and private communication.
- ²²M. Aiga and J. Itoh, *J. Phys. Soc. Japan* **31**, 1844 (1971).
- ²³A. Arima and H. Horie, *Progr. Theoret. Phys.* **12**, 623 (1954).
- ²⁴M. F. Martin, *Nucl. Data* **B6**(No. 3), 387 (1971).
- ²⁵H. Ton, G. H. Dulfer, J. Brasz, R. Kroondijk, and J. Blok, *Nucl. Phys.* **A153**, 129 (1970).
- ²⁶R. F. Petry, R. A. Naumann, and J. S. Evans, *Phys. Rev.* **174**, 1441 (1968).
- ²⁷J. C. Cunnane, R. Hochel, S. W. Yates, and P.-J. Daly, private communication to D. A. S.

Study of ^{173}Hf Levels Populated in the Decay of ^{173}Ta

I. Rezanka, I. M. Ladenbauer-Bellis, T. Tamura,* and W. B. Jones
Heavy Ion Accelerator Laboratory, † Yale University, New Haven, Connecticut 06520
 and

F. M. Bernthal

Departments of Chemistry ‡ and Physics and Cyclotron Laboratory, § Michigan State University, East Lansing, Michigan 48823,
and Heavy Ion Accelerator Laboratory, † Yale University, New Haven, Connecticut 06520

(Received 16 October 1972)

The decay of ^{173}Ta was studied using high resolution Ge(Li), Si(Li), and Si surface-barrier detectors in singles and coincidence modes. The ^{173}Ta activity was produced via the reaction $^{165}\text{Ho}(^{12}\text{C}, 4n)^{173}\text{Ta}$, at a carbon beam energy of 6.3–6.9 MeV per nucleon. All spectra were obtained from chemically separated Ta sources. Besides the previously known energy levels of ^{173}Hf , the following levels in keV were determined: 255.5, 451.9, 508.9, 635.8, 775.5, 785.3, 811.7, 927.5, 942.5, 1020.3, 1111.4, 1127.0, 1192.8, 1248.3, 1450.0, 1574.2, 1655.6, 1667.1, 1694.3, and 2263.3. Rotational bands based on the $(1/2)^- [521]$ (g.s.), $(5/2)^- [512]$ (107.2 keV), and $(7/2)^+ [633]$ (197.5 keV) Nilsson states were observed. The half-lives of the $(5/2)^- [512]$ and the $(1/2)^+ [633]$ band heads were determined to be (182 ± 20) nsec and (160 ± 40) nsec, respectively. The probability of the radiative $E1$ transition between the $[633]$ and $[512]$ band heads was calculated within the framework of Nilsson model including the pairing and Coriolis interactions. From measurement of the β^+ end-point energy, the mass difference between ^{173}Ta and ^{173}Hf was determined to be 3670 ± 200 keV.

1. INTRODUCTION

In-beam γ -ray spectroscopic studies have recently revealed substantial deviations from the strong coupling model^{1,2} in the even-parity bands of odd-neutron deformed nuclei in the rare-earth

region. This development initiated new interest in the investigation of the level structure of these nuclei as populated in radioactive decay. The quieter environment of radioactivity experiments as compared with the in-beam work enables one to perform experiments crucial for the confirma-